Energy & Environmental Science

ROYAL SOCIETY OF CHEMISTRY

PAPER

View Article Online
View Journal | View Issue

Cite this: *Energy Environ. Sci.*, 2026, **19**, 2900

Bio-based encapsulation materials enabling recyclable and stable perovskite solar cells

Chengda Ge,[a] Yingying Liu,[b] Rui Wang,*[b] Lei Song,[b] Xiang Deng,[c] Gengxin Du,[a] Yidan An,[a] Lingyi Ke,[a] Yiting Jiang,[d] Tingfeng Lei,[a] Quanrun Qiu[a] and Hin-Lap Yip*[adef]

Perovskite solar cells (PSCs) are considered a promising next-generation photovoltaic technology due to their high power conversion efficiency and cost-effective manufacturing. However, their practical application is hindered by the lack of suitable encapsulation materials that protect against environmental degradation while maintaining compatibility with the chemical and thermal fragility of metal halide perovskites. Conventional encapsulation materials, such as ethylene-vinyl acetate (EVA) copolymer and polyolefin elastomer (POE) films, rely on high processing temperatures (>140 °C) and reactive additives, which can damage PSCs during encapsulation. Developing environmentally friendly, low-temperature encapsulation materials tailored to PSCs is therefore critical to advancing their industrialization. Here, we present a bio-based fluorinated polyether ester (PTFF) polymer film as a recyclable and nondestructive encapsulation solution for PSCs. PTFF, synthesized mainly from biomass-derived monomers, achieves additive-free adhesion through noncovalent interactions and features a tunable glass transition temperature (<80 °C) for low-temperature hot-pressing. Encapsulated PSCs demonstrate excellent thermal and moisture stability, retaining >80% efficiency after 600 hours under damp heat conditions (85 °C, RH = 85%). Moreover, PTFF is easily recyclable *via* simple physical delamination methods, maintaining its adhesion performance after recovery. This work highlights a sustainable encapsulation strategy tailored to PSCs, addressing their unique stability and environmental requirements, and provides a pathway toward scalable and sustainable photovoltaic module production.

Received 25th November 2025,
Accepted 9th April 2026

DOI: 10.1039/d5ee07173a

rsc.li/ees

Broader context

In the process of perovskite solar cells (PSCs) moving towards practical applications, effective encapsulation is crucial for extending their lifespan and preventing potential lead leakage. Developing environmentally friendly encapsulation materials compatible with traditional lamination processes and suitable for PSCs is of great significance for advancing the application of PSCs and improving the environmental attributes of PSC modules. In this work, we develop a new kind of bio-based material PTFF for PSC encapsulation, which exhibits superior barrier properties and operational resilience, with stability assessments under accelerated aging protocols—including damp heat (85 °C/85% RH), thermal cycling (−40 °C to 85 °C), and maximum power point (MPP) tracking—validating its exceptional protective efficacy. Encapsulated devices maintain high power conversion efficiency (PCE) retention across all stressors, demonstrating reliable barrier functionality under extreme operational environments. Collectively, this work establishes PTFF as a triple-objective enabler: scalable processing compatibility, end-of-life recyclability, and uncompromised environmental compliance—providing a promising industrialization pathway for perovskite photovoltaics.

[a] *Department of Materials Science and Engineering, City University of Hong Kong, Kowloon, Hong Kong 999077, China. E-mail: a.yip@city.edu.hk*
[b] *Division of Energy Materials (DNL 22), Dalian Institute of Chemical Physics of the Chinese Academy of Sciences, Dalian 116023, China. E-mail: wangrui87@dicp.ac.cn*
[c] *Guangdong Mingyang Thin Film Technology Co., Ltd, Zhongshan, China*
[d] *School of Energy and Environment, City University of Hong Kong, Kowloon, Hong Kong 999077, China*
[e] *Hong Kong Institute for Clean Energy, City University of Hong Kong, Kowloon, Hong Kong 999077, China*
[f] *State Key Laboratory of Marine Environmental Health, City University of Hong Kong, Kowloon, Hong Kong, 999077, China*

Introduction

Perovskite solar cells (PSCs) exhibit significant application potential due to their rapidly increasing power conversion efficiency (PCE),[1–3] low manufacturing costs,[4–6] and solution processability.[7,8] While manufacturing processes and device efficiency have advanced considerably,[9] stability and sustainability challenges now represent the primary obstacles to the practical deployment of PSCs.[10–14] Recent strategies—including

composition engineering, interface engineering, and additive engineering—have substantially improved device stability,[15–18] thereby enhancing practical viability. Furthermore, recycling methods using water-based green solvents have demonstrated enhanced environmental sustainability for PSC modules.[14] Beyond intrinsic device stability, developing efficient and eco-friendly encapsulation technologies is critical for establishing robust moisture/oxygen barriers, extending operational lifespans, and enabling end-of-life component recycling.

For laboratory-scale PSC encapsulation, UV-curable adhesives (UVCAs) are frequently utilized. However, direct contact between UVCAs and perovskite layers must be avoided due to the risk of UV-induced decomposition or chemical reactions that degrade perovskite integrity.[19] Additionally, UVCA encapsulation faces scalability limitations for large-area PSCs owing to equipment costs, process control requirements, and challenges in achieving uniform curing coverage. Within industrial photovoltaics, hot-lamination of polymer encapsulation films is the primary method employed, not only to enhance the mechanical stability of modules but also to significantly reduce water and oxygen permeation, thereby ensuring prolonged durability and optimal performance.[20,21] Standard encapsulant films like ethylene-vinyl acetate copolymer (EVA) and polyolefin elastomers (POE) substantially enhance module longevity.[22,23] Critically, these materials exhibit inherently weak adhesion and rely on incorporating chemically active additives—such as silane coupling agents and organic peroxides—to achieve sufficient bonding between substrates and cover glass.[24–26]

While highly effective for crystalline silicon (c-Si) solar cells due to their thermal stability, conventional hot-pressing processes (>140 °C)[27–29] combined with reactive additives preclude non-destructive encapsulation for most PSCs. This limitation arises from the thermal instability of organic charge transport layers and typical perovskite compositions, requiring specialized thermally robust perovskites or indium tin oxide (ITO) top electrodes for compatibility.[30]

Growing research interests are directed towards developing advanced encapsulation solutions to bridge the lab-to-fab gap for perovskite photovoltaics. Emerging encapsulants—including polyurethane,[31] phase-change waxes,[32] self-healing epoxies,[33] low-migratory UVCAs,[19,34] and bioadhesives[35]—demonstrate promising moisture barrier properties and perovskite compatibility. Similarly, high-performance barrier technologies like plasma-enhanced atomic layer deposition (PE-ALD) and laser-assisted glass-frit sealing[36,37] have achieved ultralow water vapor transmission rates ($<10^{-4}$ g m^{-2} day^{-1}). However, these approaches face critical limitations: novel materials typically require non-scalable processing methods, while advanced techniques necessitate prohibitively expensive capital equipment. Consequently, industrially viable encapsulation for PSCs requires materials compatible with standard hot-lamination processes (<100 °C), free of reactive additives, and inherently sustainable.

Herein, we report a bio-based fluorinated polyether-ester (PTFF) designed specifically for perovskite encapsulation. Synthesized *via* copolymerization of 2,5-furandicarboxylic acid (FDCA) and tailored polyols, PTFF achieves precise control over polyether/polyester segment ratios, enabling tunable glass transition temperatures through feed ratio manipulation. Crucially, PTFF forms robust substrate adhesion *via* multifunctional supramolecular bonding (hydrogen bonding, electrostatic, and van der Waals interactions) between polymer chain functionalities and substrate oxides, eliminating the need for chemically active additives. This additive-free encapsulant enables two transformative advantages: (1) non-destructive encapsulation of thermally sensitive PSCs and (2) closed-loop recyclability *via* a mild physical recycling method—outperforming permanent crosslinks in EVA/POE systems.

Moreover, PTFF exhibits superior barrier properties and operational resilience, with stability assessments under accelerated aging protocols—including damp heat (85 °C/85% RH), thermal cycling (−40 °C to 85 °C), and maximum power point (MPP) tracking—validating its exceptional protective efficacy. Encapsulated devices maintain high PCE retention across all stressors, demonstrating reliable barrier functionality under extreme operational environments. Collectively, this work establishes PTFF as a triple-objective enabler: scalable processing compatibility, end-of-life recyclability, and uncompromised environmental compliance—providing a promising industrialization pathway for perovskite photovoltaics.

Results and discussion

Design principles

Traditional EVA/POE encapsulation methods present three critical challenges for PSCs: (1) adhesion dependence on reactive additives, (2) high processing temperatures exceeding 140 °C, and (3) reliance on petroleum-derived monomers, conflicting with global carbon neutrality goals. Addressing these limitations necessitates sustainable encapsulation alternatives to reduce the carbon footprint of photovoltaic manufacturing.

Effective hot-pressing encapsulation for PSCs requires additive-free formulations and low-temperature processing. Guided by these requirements and environmental sustainability, we selected bio-based monomers—FDCA and polyols—to fabricate polymeric encapsulation films. Unlike petroleum-based monomers in EVA and POE, FDCA and polyols are sustainably sourced from biomass. The heteroatom-containing aromatic structure of FDCA enables noncovalent interactions (*e.g.*, oxygen binding, π–metal interactions, and hydrogen bonding[38–41]), permitting intrinsic adhesion without high-activity additives used in conventional films. While polar oxygen atoms in FDCA enhance adhesion, they may compromise water barrier properties. To mitigate this, we further incorporated fluorine-rich 2,2,3,3,4,4,5,5-octafluoro-1,6-hexanediol (OFHDO) into the polymer design to increase the hydrophobicity of the polyether-ester matrix. These design principles are summarized in Fig. 1a.

Polymer synthesis and characterization

After establishing the adhesion mechanism, we prioritized reducing processing temperatures by controlling the glass

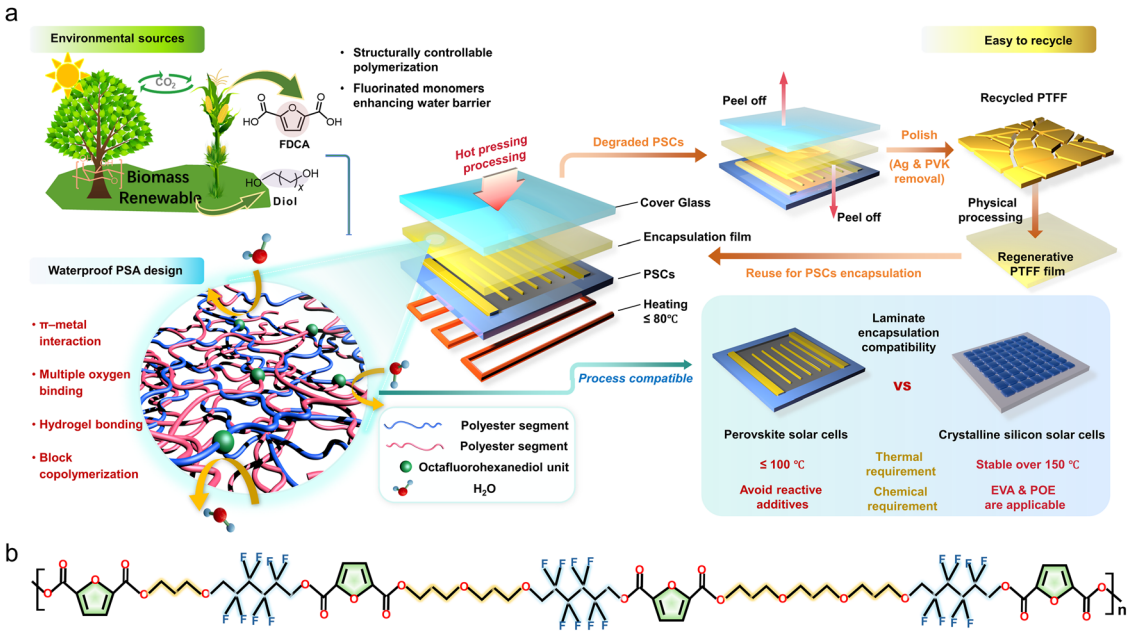

Fig. 1 Synthesis of PTFF and product screening. (a) Design principle of recoverable PTFF for PSCs nondestructive encapsulation. (b) Molecular structure of PTFF.

transition temperature (T_g) of the polymer *via* structurally controlled polymerization. Using rare-earth catalysts, we synthesized block copolymers through a one-pot reaction. Unlike traditional polyester synthesis, strong electron-withdrawing ligands and rare-earth ions enabled directional polymerization, yielding block polymers with coexisting polyester and polyether segments (reaction mechanism: Fig. S1; structure: Fig. 1b).

The coexistence of rigid (polyester) and flexible (polyether) segments allowed precise control of T_g by adjusting segment ratios *via* reaction conditions, while retaining the excellent water barrier properties of the polyester. We synthesized multiple PTFF samples under varied conditions (Table S1). Nuclear magnetic resonance hydrogen (^{1}H NMR) spectroscopy confirmed the chemical structures and quantified segment ratios (Fig. S1b). As anticipated, reaction parameters successfully tuned segment proportions (Table S1).

Differential scanning calorimetry (DSC) revealed that increasing the proportion of polyether segments reduced T_g (Fig. S1c), enhancing the thermal motion of polymer chains and facilitating functional group bonding with the substrate at lower processing temperatures. For samples with low T_g, water contact angle measurements (Fig. S3) confirmed that hydrophobic properties imparted by the OFHDO monomer counteracted hydrophilic ether bonds, reducing surface energy of the polymer and increasing the water contact angle—critical for improving water resistance of PTFF. Given the highest water contact angle and the lowest T_g in PTFF sample #1, we selected it for further characterization and subsequent experiments. The collected PTFF particle material after the polymerization reaction was filled between two polyimide films and further processed into thin films with a thickness of 0.45 mm (same as commercial POE and EVA films) through hot pressing (120 °C, 5 Mpa for 30 s) for subsequent hot-lamination assessment of PSCs.

Adhesion assessment of PTFF

Based on the selected PTFF film, we systematically evaluated its adhesion properties and underlying encapsulation mechanisms. For solar cell encapsulation, robust interfacial adhesion between the substrate and the cover glass is critical to withstand mechanical stress and prevent environmental degradation due to water and oxygen infiltration. Processing temperature and duration during hot pressing are equally vital parameters, directly impacting both perovskite layer integrity and energy consumption during the industrial encapsulation process.

We assessed adhesion performance through shear-tensile testing (Fig. 2a) with simultaneous work-of-debonding calculations.[42] Commercial EVA, POE, and our PTFF films of identical dimensions were hot-pressed between standardized substrates under controlled pressure while systematically varying temperature (60–150 °C) and holding time (1–5 min). Temperature optimization at fixed holding time revealed optimal adhesion for EVA at 140 °C and POE at 150 °C (Fig. 2b and c and Fig. S4), consistent with literature values.[27–29] However, these temperatures are too high for PSCs, which are thermally sensitive.

In contrast, PTFF achieved excellent adhesion at just 60 °C, and its performance at 80 °C exceeded that of EVA and POE, with a work of debonding (263 N m^{-1}) that is one order of magnitude higher than those of commercial benchmarks (20.1 N m^{-1} of EVA at 140 °C/13.2 N m^{-1} of POE at 155 °C) (Fig. 2d). This low processing temperature makes PTFF suitable for PSCs. We then optimized the holding time by varying the hot-pressing duration at the optimal temperatures and

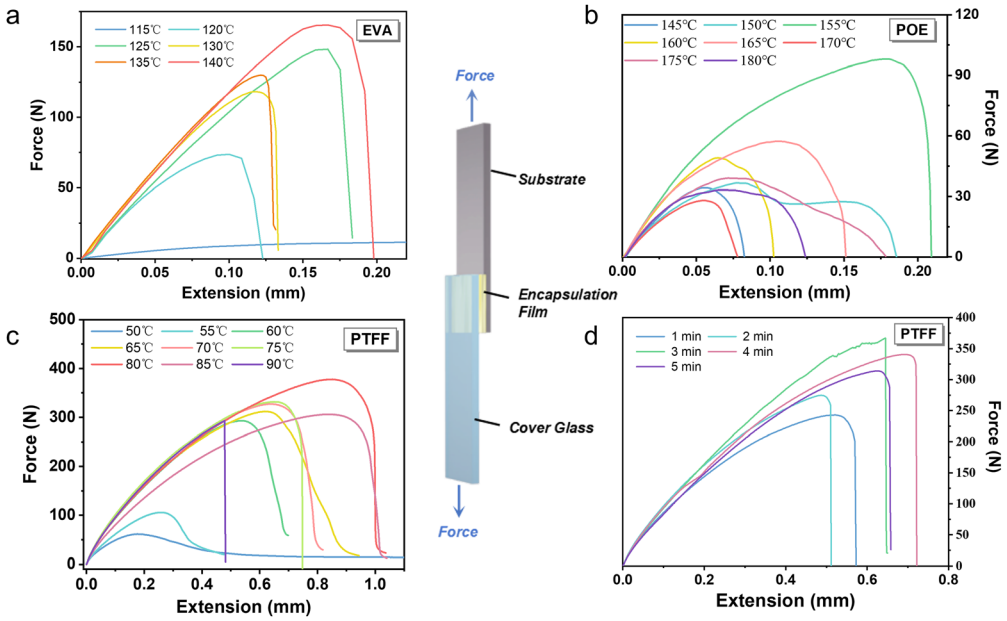

Fig. 2 Comparative evaluation of the adhesive strength of different encapsulation materials *via* shear tensile experiments. Stress–strain curves of (a) EVA, (b) POE and (d) PTFF obtained from shear tensile experiments with variable hot-pressing temperatures. (d) Stress–strain curves of variable holding times of PTFF with a fixed optimal hot-pressing temperature.

calculated the work of debonding (Fig. S5). As shown in Fig. 2d, the optimal holding time for PTFF was 3 minutes, similar to EVA (2 minutes) and POE (3 minutes), indicating minimal energy consumption. This minimal duration, combined with its 60–80 °C processing window *versus* 140–150 °C for commercial films, allows PTFF-based lamination technology to operate with reduced energy input, thereby contributing to its environmentally friendly and energy-efficient attributes.

Beyond adhesion, water vapor transmission rate (WVTR) is another critical parameter for encapsulation. The aromatic furan rings in PTFF improve substrate interaction and enhance water vapor and solvent barrier properties.[38,41] WVTR testing (Table S2) showed that the WVTR of PTFF was lower than that of EVA but slightly higher than that of POE at room temperature. However, at elevated temperatures (55 °C), the WVTR of PTFF (30.829 g m^{-2} day^{-1}) approached that of POE (26.684 g m^{-2} day^{-1}) and remained much lower than EVA (149.470 g m^{-2} day^{-1}), demonstrating strong water vapor resistance suitable for PSC encapsulation.

To simulate the potential solvent corrosion that encapsulation materials may encounter in practical applications, we exposed the encapsulation polymers to common solvents and evaluated their adhesive performance after aging (Fig. S6 and Table S3). PTFF demonstrated excellent solvent tolerance, attributed to its additive-free design and unique molecular structure. Notably, PTFF exhibited enhanced adhesion after seawater aging, likely due to polymer recrystallization induced by the motion of fluorine-containing monomers in poor solvents. This behavior highlights the exceptional salt resistance of PTFF and its potential for underwater photovoltaic encapsulation.[43,44]

To evaluate its performance under wet conditions, we conducted underwater load-shear experiments, which confirmed the reliability of the underwater bonding properties of PTFF (Fig. S7). PTFF also demonstrated exceptional long-term durability, maintaining outstanding stability even after a three-month solvent aging test (Fig. S8 and Table S4). These results highlight the ability of PTFF to withstand harsh environments, including prolonged exposure to corrosive conditions.

In sharp contrast, EVA and POE showed significant adhesion degradation after solvent aging. This loss of performance is likely due to the deactivation of their additives in solvent environments, exposing a critical limitation of these traditional materials. Moreover, the solvent aging tests revealed an additional advantage of PTFF: its additive-free design eliminates the need for strict temperature and humidity controls during storage. Unlike EVA and POE, which require specialized storage conditions (temperature of 22 °C and a relative humidity $\leq$50%)[45] to maintain their properties, PTFF retains its performance without such requirements. This unique feature not only enhances the practicality of PTFF but also significantly reduces the production and operational costs, making it a more sustainable and cost-effective solution for industrial applications.

Adhesive mechanism of PTFF

In the Design principles section, we emphasized that, in contrast to conventional encapsulation materials such as EVA and POE, the PTFF polymer was specifically engineered with an additive-free design. The strong adhesion of PTFF to the substrate and cover glass is facilitated by intensive noncovalent interactions, which are critically different from the chemical

bonding mechanisms typically employed in traditional encapsulation films.

To validate the presence of these noncovalent interactions-based bonds, Fourier Transform Infrared (FTIR) spectroscopy was employed to examine the interactions between the functional groups in PTFF and the substrate. In PSCs, the exposed substrate surface at the device edges, resulting from the etching process, is a critical interface for preventing water and oxygen ingress. In the p–i–n structured devices studied herein, the common exposed surface typically comprises indium tin oxide (ITO) and nickel oxide (NiO_x). FTIR spectra of PTFF and its mixtures with ITO and NiO_x (Fig. 3a and b) revealed notable shifts in the characteristic ester peaks (C=O at 1714 cm^{-1} and C–O–C at 1283 cm^{-1}),[46,47] and in the ether stretching peak (C–O–C at 1105 cm^{-1})[48] after contact with the two metal oxides, consistent with multiple metal-ion-oxygen coordination effects. Meanwhile, the furan-ring bending mode at 955 cm^{-1} and the ring-breathing mode at 1015 cm^{-1} (ref. 49 and 50) also shift, suggesting strong π-metal interactions between the furan units and the metal oxides.

For recyclable encapsulation, the pressure-sensitive adhesive (PSA) effect is a particularly desirable property. PSA allows the polymer to strongly bond to substrates under mild pressure and temperature, avoiding the use of additives or irreversible chemical crosslinking that hinders recycling. At the same time, PSA enables peelability after cooling or embrittlement, which is critical for recovering device components without damaging them. To evaluate PSA behavior, dynamic mechanical analysis (DMA) is widely applied, since the storage modulus (G'), loss modulus (G''), and their temperature or frequency dependence directly reveal the balance between rigidity, toughness, and viscous flow that governs adhesion and recyclability. In this context, the unique adhesion of PTFF can be understood as arising from its additive-free design and PSA-driven interfacial interactions.

We therefore further investigated potential changes in physical properties and the rheological behavior of the adhesives during operation using DMA. First, we evaluated the modulus of the encapsulation materials as a function of temperature at a fixed step time and oscillation frequency. From the temperature sweep (20–80 °C) in Fig. 4b, once the temperature exceeds ~45 °C, G' for PTFF drops below the Dahlquist criterion ($G' \leq 3 \times 10^5$ Pa), indicating the onset of pressure-sensitive adhesive (PSA) behavior.[51] The maximum in the loss factor ($\tan\delta$) at ~28 °C marks the transition to more viscous behavior and closely corresponds to T_g, underscoring the importance of lowering T_g to enable low-temperature hot pressing. For the benchmark encapsulants POE and EVA, EVA behaves as a PSA across the entire temperature range, whereas POE does not—consistent with its previously reported higher hot-pressing temperature. We then conducted time- and frequency-dependent experiments to characterize viscoelastic behavior in more detail. The time-dependent rheological test reveals that PTFF exhibits comparable G' and G'' moduli, indicating a balance of rigidity and toughness—aligned with our design principle of integrating rigid and flexible segments within one material.

We next performed frequency-dependent DMA to obtain G' and G'' (Fig. 5a–c) and constructed viscoelastic windows[52] to analyze and compare adhesive behavior (principles of viscoelastic window analysis are elaborated in Fig. S9). As shown in Fig. 5d, the application window of PTFF lies in quadrant 3, characteristic of a peelable PSA. Notably, the viscoelastic window of PTFF is very small, indicative of high shear strength. This likely arises from a flatter rubbery plateau, reflecting greater chain entanglement or physical cross-linking in PTFF. In contrast, EVA falls in quadrant 1 and behaves as a low-viscosity elastomer, *i.e.*, effectively non-PSA, whereas POE sits at the junction of quadrants 1 and 3, implying temperature-dependent transitions among PSA states. The viscoelastic windows also suggest that the intrinsic adhesion of POE and EVA is insufficient for robust substrate bonding, highlighting the critical role of additives in their adhesion performance.

Device encapsulation efficacy of PTFF

To assess the practical effectiveness of PTFF for hot-press encapsulation of PSCs, we carried out device encapsulation

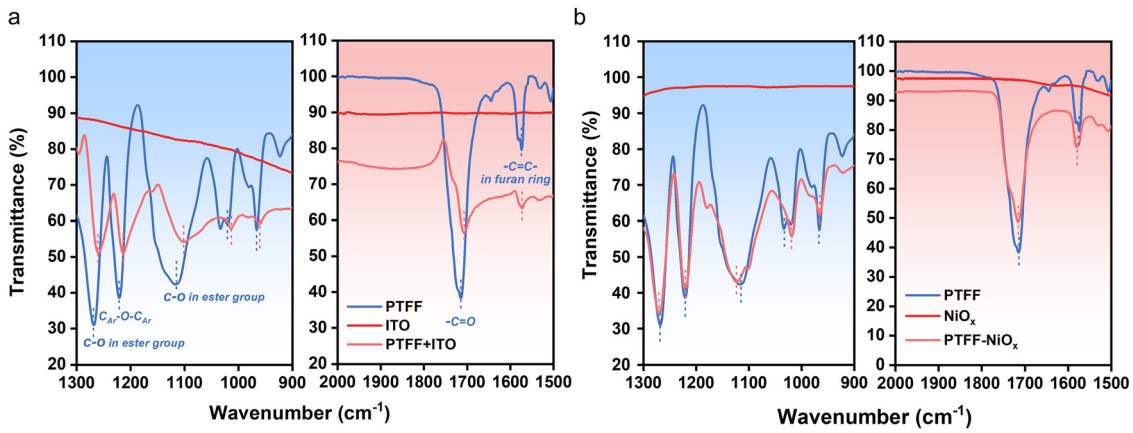

Fig. 3 Interaction between PTFF and substrates at the contact surface evidenced by FTIR. (a) FTIR spectra of PTFF, ITO and their mixture. (b) FTIR spectra of PTFF, NiO_x and their mixture.

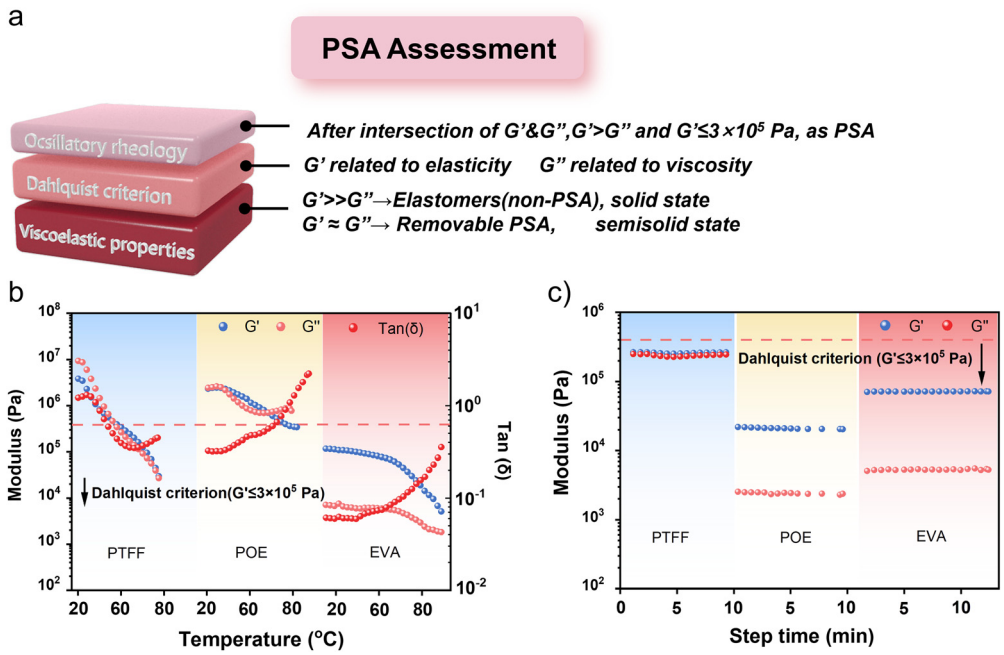

Fig. 4 Analysis of the viscoelastic behavior of encapsulation films based on DMA. (a) Key Physical parameters in PSA assessment. (b) G' and G'' of PTFF, POE, and EVA obtained from temperature-dependent DMA (ω = 1 Hz, γ = 0.1%, heating rate is 3 °C min^{-1}). (c) Time-dependent rheological test of PTFF, POE, and EVA (maintaining 25 °C for 10 min, ω = 1 Hz, γ = 0.1%).

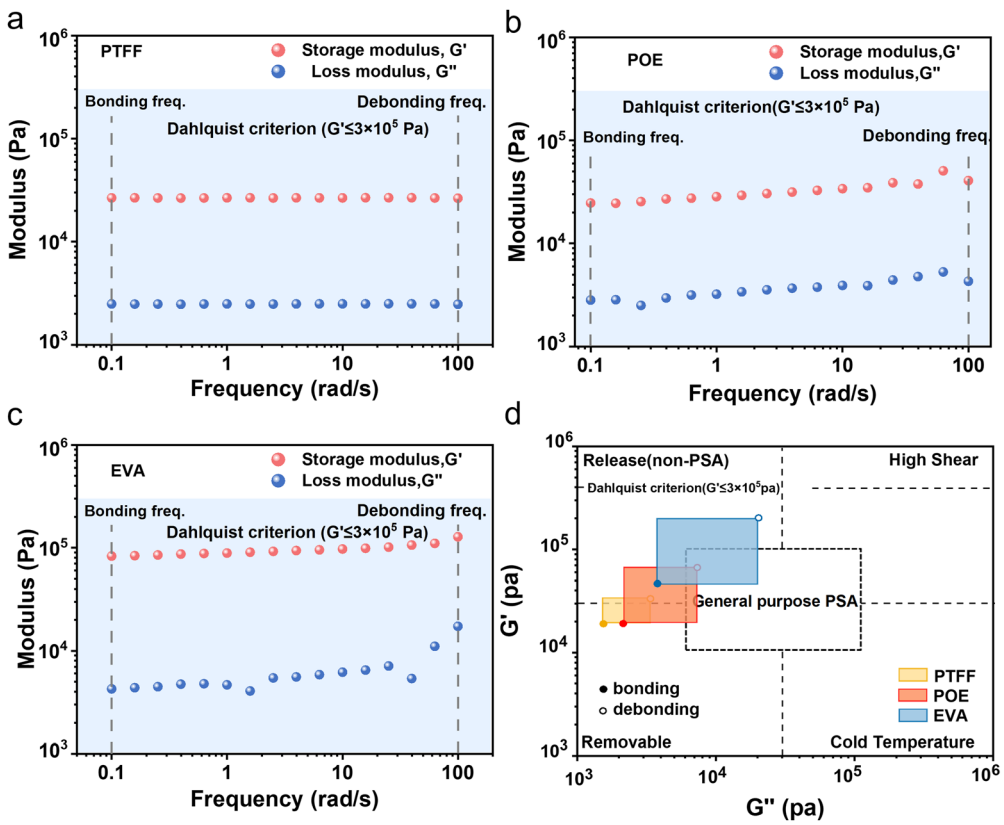

Fig. 5 Analysis of polymer applications based on viscoelastic window. G' and G'' of (a) PTFF, (b) POE and (c) EVA obtained from frequency dependent DMA (25 °C, γ = 0.1%,). (d) The corresponding viscoelastic window analysis of PTFF, POE and EVA.

and accelerated aging under damp-heat conditions. A multilayer lamination method at 80 °C was used, and device performance before and after hot pressing is shown in Fig. 6a and Fig. S10. The PCE of both 10 × 10 cm^2 minimodules (53.0 cm^2 aperture) and small-area devices changed negligibly upon encapsulation, demonstrating nondestructive processing. For reliability under extreme environments, we conducted damp-heat testing (85 °C, RH ~85%). Owing to the additive-free design and effective barrier properties, PTFF-encapsulated devices exhibited no visible degradation after prolonged damp-heat exposure. In sharp contrast, devices encapsulated with EVA and POE exhibited a change in color from black to yellow (Fig. 6b and c), indicating severe degradation. Although the EVA polymer itself is reported to be benign toward the perovskite layer,[53] this degradation likely arises because EVA and POE contain various additives[24–26,54] that can react with the active layer, and because polar additives can promote water–vapor adsorption at the polymer surface, thus accelerating corrosion. To probe water uptake by additive-containing films, we conducted thermogravimetric analysis coupled with mass spectrometry (TGA–MS). As shown in Fig. S11, at 100 °C for over 2 h, PTFF, EVA, and POE showed no decomposition of their own constituents; however, MS detected a small amount of water from EVA, consistent with additive-mediated water adsorption and underscoring the need for controlled temperature/humidity storage of additive-containing films in manufacturing. These results also confirm the thermal stability and water-resistant surface of PTFF.

To establish the context for our stability evaluations, Fig. S12 illustrates the precise lamination and encapsulation methods used, detailing the critical layering and alignment for optimal performance. Building on this, we assessed the durability of PTFF-encapsulated devices under damp-heat aging and thermal cycling. As shown in Fig. 6d and e, devices maintained over 80% of their initial PCE after more than 600 hours of damp-heat exposure and over 90% after 180 thermal cycles and 550 hours of MPP tracking. These results highlight the effectiveness of our encapsulation technique in protecting devices against harsh environmental conditions.

Recyclability of PTFF

With global emphasis on sustainability, end-of-life recycling of photovoltaic modules has become imperative. Recovering the perovskite layer is essential for mitigating lead leakage,[14] while recycling and reusing polymeric encapsulants help reduce plastic pollution. Here, the PSA nature of PTFF plays a decisive role: adhesion is strong enough for long-term device sealing but remains reversible under cooling or heating, enabling controlled peeling and recovery. In contrast, conventional encapsulants such as EVA and POE lose PSA behavior after processing because of additive-induced crosslinking, making them difficult to recycle.[55–57] Even then, reusing the recovered material as encapsulant typically requires reintroducing additives. By contrast, our bio-based PTFF is a linear, additive-free polymer that can potentially be recovered and reused *via* simple physical processes.

To demonstrate recyclability, we embrittled the PTFF layer by liquid-nitrogen cooling and then peeled it from the encapsulated PSC module (Fig. 7c); a similar outcome can be achieved by high-temperature softening followed by peeling. This peelability is a direct manifestation of the balanced viscoelastic properties revealed by DMA, linking adhesion strength with reversibility. Perovskite and silver residues on the polymer surface were removed by polishing with 800-grit

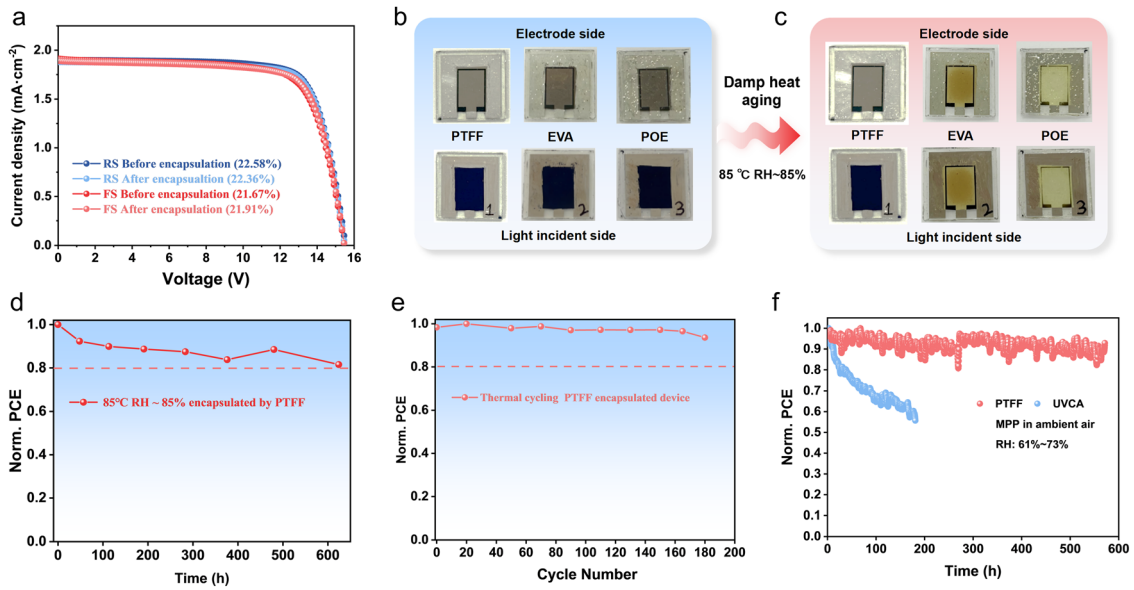

Fig. 6 The impact of encapsulation on device performance. (a) Performance of the PSC module before and after encapsulation by PTFF. (b) Devices encapsulated by PTFF, EVA, and POE before damp-heat aging. (c) Devices after damp-heat aging in (b). (d) The performance of the PTFF encapsulated device during the damp heat aging test. (e) Performance of the PTFF encapsulated device during the thermal cycling aging test. (f) MPP tracking of devices encapsulated by different materials.

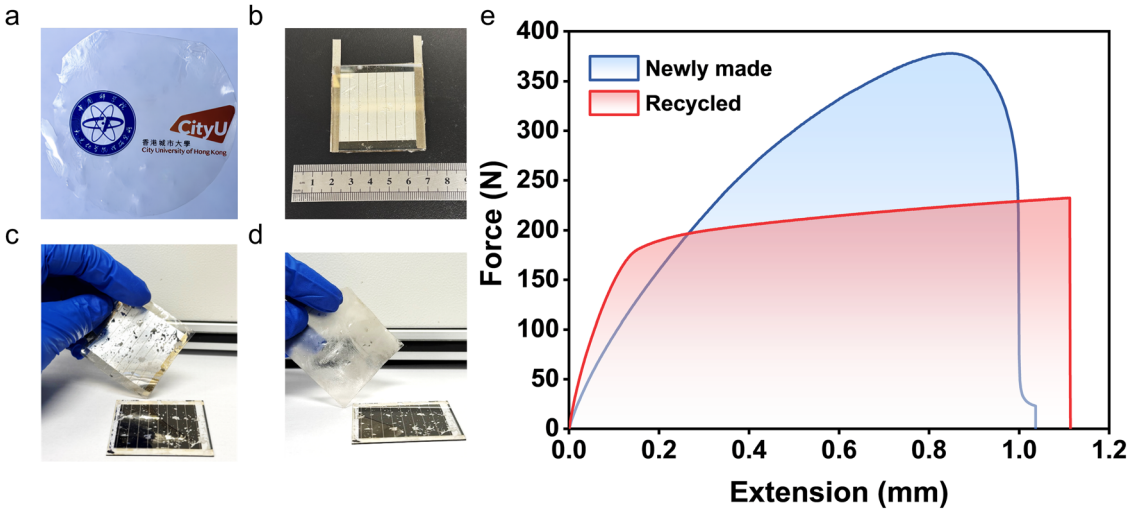

Fig. 7 Evaluation of the recyclable performance of PTFF. (a) Original PTFF encapsulation film. (b) Electrode side display of the PSC module encapsulated based on PTFF lamination technology. (c) The PTFF film recycled by the peeling off method. (d) The recycled PTFF film (c) treated by 800 grit sandpaper polishing. (e) Comparison of shear and tensile testing between newly made PTFF and recycled PTFF.

sandpaper (Fig. 7d). The recovered PTFF was hot-pressed into a thin film, and its adhesion performance was evaluated *via* the previously described shear–tensile test. As shown in Fig. 7e, the recycled PTFF still maintains its strong adhesive strength (exceeding 91% of the initial detachment work) compared to that of the as-prepared film; detailed mechanical parameters are provided in Table S5, with statistics over multiple samples in Table S6, corroborating facile recyclability.

In addition to evaluating the mechanical properties of PTFF, we also explored its reusability for device encapsulation. SEM images in Fig. S13 and S14 visually confirm the surface integrity of PTFF before and after recycling, demonstrating that the recycling process preserves the quality of the film without harming the encapsulated devices. We then further assessed the performance of a monitoring device before and after encapsulation with recycled PTFF to demonstrate the viability of our closed-loop recycling design. As illustrated in Fig. S15–S18, the recycled PTFF continues to provide effective protection for the device. By stark contrast, EVA and POE entirely lost adhesion after the same recycling protocol, preventing bonding to substrates and precluding stress–strain measurements. To confirm that heavy metals (Ag, Pb) do not contaminate the recycled PTFF, we performed inductively coupled plasma–optical emission spectrometry (ICP–OES). As reported in Table S7, both pre-encapsulation and post-recycling PTFF contain negligible Ag and Pb, indicating that interactions between PTFF and metals in the devices are confined to the interface without diffusion into the polymer bulk.

Conclusions

Developing environmentally friendly, nondestructive encapsulation materials for PSCs is vital to practical deployment, extended device lifetimes, and mitigation of lead-leakage risks. Here, we introduce a bio-based encapsulant, PTFF, compatible with hot-pressing processes used in the current photovoltaic industry. Most PTFF monomers are bio-derived, offering a greener alternative to petroleum-based EVA and POE. The additive-free composition, strong water-barrier performance, solvent resistance, and low processing temperature (≤ 80 °C) of PTFF enable nondestructive encapsulation, robust protection under harsh conditions (damp heat and large temperature swings), and straightforward physical recycling at the end of life. This recyclability complements ongoing efforts toward environmentally responsible PSC module recycling. Overall, bio-based PTFF holds considerable potential for applications in perovskite photovoltaics, offering a promising pathway toward extending PSC service life, reducing manufacturing carbon emissions, and advancing the practical deployment of this technology.

Author contributions

H.-L. Y. and R. W. supervised the project. R. W. and C. G. conceived and initiated the project, contributed to the design and synthesis of PTFF. R. W. and Y. L. contributed to the corresponding physical and chemical properties characterization and analysis of the PTFF. C. G., L. S., R. W., and H.-L. Y. wrote the paper together. C. G. fabricated the devices and performed most of the characterization related to the evaluation of the device encapsulation. X. D. fabricated the modules and conducted laminate encapsulation of the 10 × 10 cm^2 modules. Y. A. L. K and G. D. contributed to the preparation and characterization of the devices. Y. J., T. L. and Q. Q. contributed to the characterization of the devices.

Conflicts of interest

The authors declare no competing interests.

Data availability

All data generated or analyzed during this study are included in the published article and its supplementary information (SI). Supplementary information: all additional data including Fig. S1–S18, Tables S1–S8 and supplementary text. See DOI: https://doi.org/10.1039/d5ee07173a.

Acknowledgements

Dr R. W. thanks the National Key Research and Development Program of China (2022YFC2105800) and the National Natural Science Foundation of China (NSFC) 52473012 for the financial support. Prof. H.-L. Y. acknowledges financial support from the Research Grant Council (RGC) of Hong Kong through the RGC Senior Research Fellow Scheme (SRFS 2526-1S04) and the General Research Fund (GRF No. 11307323), the NSFC/RGC Collaborative Research Scheme (CRS_CityU104/23), and the ITF grant (GHP/394/22GD) from Innovation and Technology Commission of Hong Kong. This work is supported by the State Key Laboratory of Marine Environmental Health which receives regular funding from the Innovation and Technology Commission of the Hong Kong SAR Government (PJ9448002). The work is also financially supported by the City University of Hong Kong for the project 'Fostering Innovation for Resilience and Sustainable Transformation' (FIRST), officially endorsed by the United Nations Educational, Scientific and Cultural Organization (UNESCO) under the International Decade of Sciences for Sustainable Development (IDSSD) (2024–2033) *via* the internal City University of Hong Kong account of 9610739. The authors thank Towngas Energy Academy (Shenzhen) Co., Ltd. for providing photovoltaic-grade EVA and POE encapsulation films for the damp-heat aging test of PSCs.

References

1 H. Chen, C. Liu, J. Xu, A. Maxwell, W. Zhou, Y. Yang, Q. Zhou, A. S. R. Bati, H. Wan, Z. Wang, L. Zeng, J. Wang, P. Serles, Y. Liu, S. Teale, Y. Liu, M. I. Saidaminov, M. Li, N. Rolston, S. Hoogland, T. Filleter, M. Kanatzidis, B. Chen, Z. Ning and E. H. Sargent, *Science*, 2024, **384**, 189–193.
2 C. Liu, Y. Yang, H. Chen, I. Spanopoulos, A. S. R. Bati, I. W. Gilley, J. Chen, A. Maxwell, B. Vishal, R. P. Reynolds, T. E. Wiggins, Z. Wang, C. Huang, J. Fletcher, Y. Liu, L. X. Chen, S. De Wolf, B. Chen, D. Zheng, T. J. Marks, A. Facchetti, E. H. Sargent and M. G. Kanatzidis, *Nature*, 2024, **633**, 359–364.
3 Y. Yang, H. Chen, C. Liu, J. Xu, C. Huang, C. D. Malliakas, H. Wan, A. S. R. Bati, Z. Wang, R. P. Reynolds, I. W. Gilley, S. Kitade, T. Wiggins, S. Zeiske, S. Suragtkhuu, M. Batmunkh, L. X. Chen, B. Chen, M. G. Kanatzidis and E. H. Sargent, *Science*, 2024, **386**, 898–902.
4 J. M. Ball, M. M. Lee, A. Hey and H. J. Snaith, *Energy Environ. Sci.*, 2013, **6**, 1739–1743.
5 M. He, B. Li, X. Cui, B. Jiang, Y. He, Y. Chen, D. O'Neil, P. Szymanski, M. A. Ei-Sayed, J. Huang and Z. Lin, *Nat. Commun.*, 2017, **8**, 16045.
6 Z. Yuan, L. Zhao, E. Pradhan, M. Lai, T. Zeng and Z. Yang, *CCS Chem.*, 2022, **4**, 855–863.
7 C. Zhang and N.-G. Park, *Commun. Mater.*, 2024, **5**, 194.
8 S.-G. Kim, G. C. Fish, E. Socie, A. T. Terpstra, D.-A. Park, K. Zhu, M. Grätzel, J.-E. Moser and N.-G. Park, *Joule*, 2024, **8**, 1707–1722.
9 N.-G. Park and K. Zhu, *Nat. Rev. Mater.*, 2020, **5**, 333–350.
10 Y. Miao, M. Ren, Y. Chen, H. Wang, H. Chen, X. Liu, T. Wang and Y. Zhao, *Nat. Sustainability*, 2023, **6**, 1465–1473.
11 Y. Cheng and L. Ding, *Energy Environ. Sci.*, 2021, **14**, 3233–3255.
12 T. A. Chowdhury, M. A. Bin Zafar, M. Sajjad-Ul Islam, M. Shahinuzzaman, M. A. Islam and M. U. Khandaker, *RSC Adv.*, 2023, **13**, 1787–1810.
13 D.-A. Park, C. Zhang and N.-G. Park, *ACS Energy Lett.*, 2024, **9**, 2428–2435.
14 X. Xiao, N. Xu, X. Tian, T. Zhang, B. Wang, X. Wang, Y. Xian, C. Lu, X. Ou, Y. Yan, L. Sun, F. You and F. Gao, *Nature*, 2025, **638**, 670–675.
15 T. Yang, C. Ma, W. Cai, S. Wang, Y. Wu, J. Feng, N. Wu, H. Li, W. Huang, Z. Ding, L. Gao, S. Liu and K. Zhao, *Joule*, 2023, **7**, 574–586.
16 F. Li, X. Deng, Z. Shi, S. Wu, Z. Zeng, D. Wang, Y. Li, F. Qi, Z. Zhang, Z. Yang, S.-H. Jang, F. R. Lin, S. W. Tsang, X.-K. Chen and A. K. Y. Jen, *Nat. Photon.*, 2023, **17**, 478–484.
17 J. Suo, B. Yang, E. Mosconi, D. Bogachuk, T. A. S. Doherty, K. Frohna, D. J. Kubicki, F. Fu, Y. Kim, O. Er-Raji, T. Zhang, L. Baldinelli, L. Wagner, A. N. Tiwari, F. Gao, A. Hinsch, S. D. Stranks, F. De Angelis and A. Hagfeldt, *Nat. Energy*, 2024, **9**, 172–183.
18 Y. Yang, S. Cheng, X. Zhu, S. Li, Z. Zheng, K. Zhao, L. Ji, R. Li, Y. Liu, C. Liu, Q. Lin, N. Yan and Z. Wang, *Nat. Energy*, 2023, **9**, 37–46.
19 Y. Han, S. Meyer, Y. Dkhissi, K. Weber, J. M. Pringle, U. Bach, L. Spiccia and Y.-B. Cheng, *J. Mater. Chem. A*, 2015, **3**, 8139–8147.
20 K. Aitola, G. Gava Sonai, M. Markkanen, J. Jaqueline Kaschuk, X. Hou, K. Miettunen and P. D. Lund, *Sol. Energy*, 2022, **237**, 264–283.
21 Y. Wang, I. Ahmad, T. Leung, J. Lin, W. Chen, F. Liu, A. M. C. Ng, Y. Zhang and A. B. Djurisic, *ACS Mater. Au*, 2022, **2**, 215–236.
22 S. Jiang, K. Wang, H. Zhang, Y. Ding and Q. Yu, *Macromol. React. Eng.*, 2015, **9**, 522–529.
23 M. Tiefenthaler, G. M. Wallner and R. Pugstaller, *Sol. Energy Mater. Sol. Cells*, 2024, **264**, 112602.
24 Z. Wu, Y. Shangguan, C. Zhang and Q. Zheng, *Polymers*, 2021, **13**, 4101.
25 J. Ahmed and S. Mushtaq, *Iran. Polym. J.*, 2022, **31**, 1571–1581.
26 X.-r He, R. Zhang, Q. Chen, Y.-q Rong and Z.-q Yang, *Int. J. Adhes. Adhes.*, 2014, **50**, 128–135.

27 W. Stark, M. Jaunich, W. Bohmeyer and K. Lange, *Polym. Test.*, 2012, **31**, 904–908.
28 J. H. Park and S. H. Hwang, *Polymers*, 2022, **14**, 4620.
29 Q. Wei, X. Huo, Q. Fu, T. Wang, H. Zhao, Y. Wang, J. Yang, S. Zhan, L. Zhou, S. Wang and P. Yin, *J. Mater. Chem. C*, 2022, **10**, 8972–8978.
30 R. Cheacharoen, C. C. Boyd, G. F. Burkhard, T. Leijtens, J. A. Raiford, K. A. Bush, S. F. Bent and M. D. McGehee, *Sustainable Energy Fuels*, 2018, **2**, 2398–2406.
31 Z. Fu, M. Xu, Y. Sheng, Z. Yan, J. Meng, C. Tong, D. Li, Z. Wan, Y. Ming, A. Mei, Y. Hu, Y. Rong and H. Han, *Adv. Funct. Mater.*, 2019, **29**, 1809129.
32 S. Ma, Y. Bai, H. Wang, H. Zai, J. Wu, L. Li, S. Xiang, N. Liu, L. Liu, C. Zhu, G. Liu, X. Niu, H. Chen, H. Zhou, Y. Li and Q. Chen, *Adv. Energy Mater.*, 2020, **10**, 1902472.
33 Y. Jiang, L. Qiu, E. J. Juarez-Perez, L. K. Ono, Z. Hu, Z. Liu, Z. Wu, L. Meng, Q. Wang and Y. Qi, *Nat. Energy*, 2019, **4**, 585–593.
34 T. Wang, J. Yang, Q. Cao, X. Pu, Y. Li, H. Chen, J. Zhao, Y. Zhang, X. Chen and X. Li, *Nat. Commun.*, 2023, **14**, 1342.
35 G. Zhang, Y. Zheng, H. Wang, G. Ding, F. Yang, Y. Xu, J. Yu and Y. Shao, *Joule*, 2024, **8**, 496–508.
36 H. Wang, Y. Zhao, Z. Wang, Y. Liu, Z. Zhao, G. Xu, T.-H. Han, J.-W. Lee, C. Chen, D. Bao, Y. Huang, Y. Duan and Y. Yang, *Nano Energy*, 2020, **69**, 104375.
37 S. Emami, J. Martins, D. Ivanou and A. Mendes, *J. Mater. Chem. A*, 2020, **8**, 2654–2662.
38 F. A. Kucherov, E. G. Gordeev, A. S. Kashin and V. P. Ananikov, *ACS Appl. Mater. Interfaces*, 2020, **12**, 45394–45403.
39 M. Montejo, A. Navarro, G. J. Kearley, J. Vazquez and J. JesusLopez-Gonzalez, *J. Am. Chem. Soc.*, 2004, **126**, 15087–15095.
40 H. Wang, X. Shi, Y. Xie, S. Gao, Y. Dai, C. Lai, D. Zhang, C. Wang, Z. Guo and F. Chu, *Cell Rep. Phys. Sci.*, 2023, **4**, 101374.
41 S. K. Burgess, R. M. Kriegel and W. J. Koros, *Macromolecules*, 2015, **48**, 2184–2193.
42 M. G. Mazzotta, A. A. Putnam, M. A. North and J. J. Wilker, *J. Am. Chem. Soc.*, 2020, **142**, 4762–4768.
43 Z. Luo, X. Zhu, H. Li, Z. Lou, Y. Li, Y. Xu, R. Li, Z. Jia, Y. Liu, Z. Wang and Q. Lin, *Sol. Energy Mater. Sol. Cells*, 2023, **262**, 112557.
44 Y. C. Tseng, L. H. Yeh, H. L. Yip and C. C. Chueh, *Small*, 2025, **21**, e2412507.
45 L. Gnocchi, A. Virtuani, A. Fairbrother, E. Annigoni and C. Ballif, *Sol. Energy Mater. Sol. Cells*, 2023, **262**, 112526.
46 A. M. Ahmed, T. P. Kainulainen, J. A. Sirvio and J. P. Heiskanen, *Biomacromolecules*, 2022, **23**, 1803–1811.
47 S. Paszkiewicz, K. Walkowiak, I. Irska, A. Zubkiewicz, P. Figiel, K. Gorący and M. El Fray, *Polymer*, 2023, **269**, 125740.
48 C. Gaina, O. Ursache, V. Gaina and C. D. Varganici, *eXPRESS Polym. Lett.*, 2013, **7**, 636–650.
49 P. Gopalakrishnan, S. Narayan-Sarathy, T. Ghosh, K. Mahajan and M. N. Belgacem, *J. Polym. Res.*, 2013, **21**, 340.
50 M. Jiang, Q. Liu, Q. Zhang, C. Ye and G. Zhou, *J. Polym. Sci. Pol. Chem.*, 2011, **50**, 1026–1036.
51 M. N. Cazenave, C. Derail, F. Leonardi, G. Marin and N. Kappes, *J. Adhesion*, 2005, **81**, 623–643.
52 G. S. Sulley, G. L. Gregory, T. T. D. Chen, L. Pena Carrodeguas, G. Trott, A. Santmarti, K. Y. Lee, N. J. Terrill and C. K. Williams, *J. Am. Chem. Soc.*, 2020, **142**, 4367–4378.
53 Z. Huang, X. Hu, C. Liu, X. Meng, Z. Huang, J. Yang, X. Duan, J. Long, Z. Zhao, L. Tan, Y. Song and Y. Chen, *Adv. Funct. Mater.*, 2019, **29**, 1902629.
54 B. Lin, C. Zheng, Q. Zhu and F. Xie, *J. Therm. Anal. Calorim.*, 2019, **140**, 2259–2265.
55 A. Bandegi, T. G. Gray, S. Mitchell, A. Jamei Oskouei, M. K. Sing, J. Kennedy, K. Miller McLoughlin and I. Manas-Zloczower, *Mater. Adv.*, 2023, **4**, 2648–2658.
56 X. Li, H. Liu, J. You, H. Diao, L. Zhao and W. Wang, *Waste Manage.*, 2022, **137**, 312–318.
57 Y. Zhao, E. M. Rettner, K. L. Harry, Z. Hu, J. Miscall, N. A. Rorrer and G. M. Miyake, *Science*, 2023, **382**, 310–314.